Physical Chemistry

Tunneling dynamics of internal rotation in the nitric acid molecule

V. A. Benderskii and E. V. Vetoshkin*

Institute of Problems of Chemical Physics, Russian Academy of Sciences, 142432 Chernogolovka, Moscow Region, Russian Federation. Fax: +7 (096) 576 4009. E-mail: bend@b5570.home.chg.ru

The Hamiltonian of internal rotation about the C_2 axis in the HNO_3 molecule and its H/D-, O^{18}/O^{16}-, and N^{15}/N^{14}-isotopomers was reconstructed using the results of quantum-chemical calculations. The Fermi resonance between the torsional ($2\nu_9$) and ONO bending (ν_5) vibrations is a characteristic feature of the molecule. Tunneling splittings in the ground and excited states were calculated using the perturbative instanton approach. Abnormally large changes in the splittings upon isotope substitution of heavy atoms are predicted.

Key words: nitric acid, potential energy surface, internal rotation, tunneling splittings.

Intensive experimental studies of internal rotation in the nitric acid molecule were carried out in the 1950—1960s. The structure of the molecule was determined from microwave spectra.[1] Detailed study[2] of vibrational spectra of its H-, D-, ^{14}N-, and ^{15}N-isotopomers showed that hindered internal rotation of the OH group, corresponding to the torsional vibration in planar stable configurations, occurs in the HNO_3 molecule. A salient feature of this molecule is resonance between the torsional and ONO bending vibrations, which is responsible for the fact that tunneling splitting of the ONO bending vibration in the first excited state (35.5 MHz) is comparable with that of the second level of torsional vibration (50.7 MHz) and far (by some orders of magnitude) exceeds the splittings of the zero (~3 kHz) and first (~2 MHz) levels of the latter.[3—7]

The aim of this work is to carry out a theoretical study of the HNO_3 molecule and its isotopomers. Tunneling splittings found for the ground and lowest excited states are in good agreement with experimental data. Changes in tunneling splittings upon isotope substitution of H (by D) and heavy nuclei are considered and anomalous isotope effects are predicted. A universal approach to description of multidimensional tunneling dynamics, called the perturbative instanton approach (PIA), has been reported earlier.[8—14]

The PIA considers tunneling dynamics in low-energy potential energy surfaces (PES) of a rather general type. The PES is constructed using $3N - 6$ generalized reactive coordinates (*i.e.*, a totality of generalized coordinates including the coordinate of transition between stable configurations) and includes (1) a one-dimensional (1D) potential for the angular tunneling coordinate ϕ and (2) a set of small-amplitude transverse coordinates (coupled with ϕ) whose frequencies, equilibrium positions, and anharmonicities depend on ϕ. Despite the relatively simple structure, such PES provide the possibility of performing calculations with a desired accuracy in the low-energy region.

Translated from *Izvestiya Akademii Nauk. Seriya Khimicheskaya*, No. 11, pp. 2052—2060, November, 1999.

1066-5285/99/4811-2029 $22.00

Hamiltonian of internal rotation in the nitric acid molecule

The PES reconstruction[11,15] is based on analysis of the symmetry of vibrations using the theory of isodynamic groups. Potential couplings between the large-amplitude vibration ϕ and the set of small transverse vibrations $\{Y\}$ have the form $f_k^{(1)}(\phi)Y_k$ and $f_{kk'}^{(2)}(\phi)Y_kY_{k'}$. Functions $f_k^{(1)}(\phi)$ are expanded into a Fourier series. If the 1D-potential for ϕ has a period of $2\pi/m$ (m = 2, 3, ...), the Fourier series contains components $m\phi$, $2m\phi$, ..., the first of which makes the main contribution to the PES. The following types of ϕY-coupling are feasible for the lowest expansion terms:

$$\begin{aligned} &C\sin(m\phi)Y + 0.5\omega^2Y^2 && \text{(Sh)},\\ &C\cos(m\phi)Y + 0.5\omega^2Y^2 && \text{(Bre)},\\ &0.5\omega^2[1 + C\cos(m\phi)/\omega^2]Y^2 && \text{(Asq)}, \end{aligned} \qquad (1)$$

where C is the potential coupling constant, ω is frequency, and Y denotes a vibration.

Two additional types of coupling appear for even m:

$$\begin{aligned} &0.5\omega^2[Y + C\cos(0.5m\phi)]^2 && \text{(Hl)},\\ &C\sin(0.5m\phi)Y + 0.5\omega^2Y^2 && \text{(Hga)}. \end{aligned} \qquad (2)$$

The symmetry of coupling is determined using correlation diagrams between irreducible representations in the point symmetry groups of both the ground and transition states and in the isodynamic group. The latter is the semi-direct product of the internal group of a nonrigid molecule and the point group for its arbitrary orientation along the minimum energy path (MEP). For the HNO_3 molecule (Fig. 1), the planar C_s-configurations are stable (the dihedral angle ϕ is equal to 0 and π); $\phi = \pi/2$ in the C_s transition state. The $C_s \otimes C_2$ isodynamic group is isomorphic to the point group C_{2v}: the elements of the $C_s \otimes C_2$ group, namely, (E, ϕ), $(C_{2z}, \phi + \pi)$, $(\sigma_{xz}, -\phi + \pi)$, and $(\sigma_{yz}, -\phi)$ are respectively equivalent to the E, C_{2z}, σ_{xz}, and σ_{yz} operations in the C_{2v} group. The correlation diagram of irreducible representations of the point groups for the ground and transition states and that of the isodynamic group is shown in Fig. 2. According to this diagram, seven A′ and two A″ vibrations for the ground state are transformed into five A_1, one A_2, two B_1, and one B_2 vibration for an arbitrary configuration and into six A′ and three A″ vibrations for the transition state. Since the product of irreducible representations of a Y vibration and the Fourier component corresponding to the type of the ϕY-coupling must be totally symmetric in the $C_s \otimes C_2$ group, the interaction between ϕ ($\phi \in A_2$) and A_1 vibrations is proportional to $Y\cos(2\phi)$, while the interaction of the former with B_1 and B_2 vibrations is respectively proportional to $Y\cos\phi$ and $Y\sin\phi$.

Thus, the PES of the HNO_3 molecule includes the 1D-potential with a period of π for the torsional tunneling coordinate, five transverse coordinates with Bre-coupling, two coordinates with Hl-coupling, and one coordinate with Hga-coupling with a period of 2π:

$$\begin{aligned} V(X,\{Y_k\}) = V_0\{&0.5[1-\cos(2\phi)] + \\ &+ \sum_{k=1}^{5}\left\{0.5C_k[1-\cos(2\phi)]Y_k + 0.5\omega_k^2Y_k^2\right\} + \\ &+ \sum_{k=6,7}0.5\omega_k^2(Y_k + C_k\cos\phi/\omega_k^2)^2 + 0.5\omega_8^2Y_8^2 + \\ &+ C_8Y_8\sin\phi\} + YY' \text{ terms}, \end{aligned} \qquad (3)$$

where V_0 is the height of the 1D-potential barrier.

In the above-listed potential, we passed from dimensional coordinates $\tilde{Y}_k$ and frequencies Ω_k to dimensionless values:

$$Y_k = \sqrt{m_k/I}\,\tilde{Y}_k, \quad \omega_k = \sqrt{2}\Omega_k/\Omega_0, \qquad (4)$$

where the frequency Ω_0 and the momentum of inertia I are parameters of the 1D-potential. Expression (3) contains no coordinates with Sh-coupling, so they are not considered below. Evaluation of coefficients $\alpha_{kk'}$ showed that the contribution from off-diagonal elements, analyzed earlier,[11] is small and only Asq-couplings should be taken into account.

For the kinetic energy operator $\hat{T}$ to be totally symmetric, the product of momenta p_ip_j and the correspond-

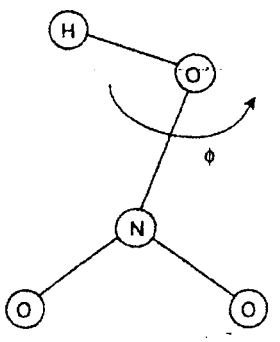

Fig. 1. Schematic view of HNO_3 molecule.

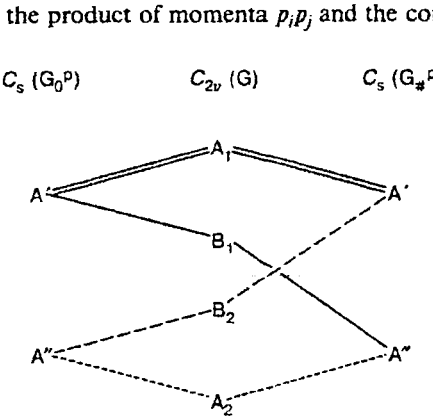

Fig. 2. Correlation diagram of irreducible representations of the point groups and the isodynamic group for HNO_3 molecule. Double lines connect irreducible representations for Bre-vibrations (with $\cos2\phi$ symmetry), solid lines connect Hl-vibrations ($\cos\phi$), long-dash lines connect Hga-vibrations ($\sin\phi$), and short-dash lines connect Sh- and T-vibrations ($\sin2\phi$).

ing Fourier component must belong to the totally symmetric representation A_1 of the $C_s \otimes C_2$ group. Taking into account that the momenta conjugate to ϕ, Bre-, Hl-, and Hga-coordinates belong to the B_2, B_1, A_1, and A_2 representations, respectively, let us write $\hat{T}$ in the form

$$\hat{T} = 0.5(1 + g_{00}\cos^2\phi)p_\phi^2 + \\ + \sum_{k=1}^{5}[0.5(1 + g_{kk}\cos^2\phi)p_k^2 + g_{0k}\sin(2\phi)p_\phi p_k] + \\ + 0.5\sum_{k=6,7}(1 + g_{kk}\cos^2\phi)p_k^2 + 0.5(1 + g_{88}\cos^2\phi)p_8^2 + \\ + g_{08}\cos(\phi)p_\phi p_8, \qquad (5)$$

where g_{ij} are dimensionless kinematic coupling constants.

Generalized coordinates can be chosen in such a way as to eliminate kinematic couplings between the coordinates belonging to the same irreducible representation, *i.e.*, to eliminate the addends proportional to $p_\phi p_{Hl}$ in formula (5). It can be easily shown that the values of terms describing kinematic couplings proportional to $p_\phi p_{Bre}$ are small. The contributions from kinematic YY'-couplings of higher orders can be neglected.[12]

The Schrödinger equation written in $(\phi, \{Y\})$-coordinates has the form

$$\left\{\frac{\partial^2}{\partial\phi^2} + \sum_{j=1}^{8}\frac{\partial^2}{\partial Y_j^2} + \right. \\ \left. + 2\gamma^2\left[\frac{\varepsilon_{n1,n2,\ldots}}{\gamma} - V(\phi,\{Y_j\})\right]\right\}\Psi(\phi,\{Y_j\}) = 0, \qquad (6)$$

where $\varepsilon_{n1,n2,\ldots} = \gamma E_{n1,n2,\ldots}/V_0$ is the dimensionless energy and

$$\gamma = I\Omega_0/(\hbar\sqrt{2}) = \sqrt{V_0 I}/\hbar \qquad (7)$$

is the parameter of semiclassical expansion.

This equation is solved using the instanton approach based on the assumption that there exists (in imaginary time) an extreme tunneling trajectory (ETT), which minimizes the semiclassical action between the potential minima. The action determines the exponent of the wave functions and, consequently, tunneling splittings. The PIA,[9–14] uses expansions in powers of the coefficients of potential and kinematic couplings when solving semiclassical Hamilton–Jacobi equations and the transport equation. The semiclassical wave functions thus found are substituted in the generalized Lifshitz–Herring formula,[10] which makes it possible to determine tunneling splittings for both the ground and lowest excited states.

Determination of parameters of the Hamiltonian

The geometry, eigenfrequencies, and eigenvectors of vibrations in the ground and transition states were obtained by the Møller–Plesset (MP2) method in the 6-311G** basis set using the GAUSSIAN-94 program.[16] The calculated ground-state geometry is in good agreement with that determined from microwave spectra[1] (Table 1). For convenience, along with the conventional numbering of vibrations in descending order of their frequencies (ν_k), from here on we will also use another numbering, namely, the 0,0-elements and the quantum number n will be associated with the tunneling coordinate while transverse vibrations Y_k (with quantum numbers n_k, $k = 1, \ldots, 8$) will be grouped by coupling symmetry in order Bre, Hl, Hga.

Parameters of the Hamiltonian defined by formulas (3) and (5) can be found using a limited set of quantum-chemical data on the geometry and normal vibrations in the ground and transition state.[17,18] Calculations of parameters of the Hamiltonian describing small vibrations of polyatomic molecules with the only stable configuration are carried out using the standard FG-formalism.[19] The presence of a large-amplitude coordinate makes the problem much more complicated. The choice of $(\phi,\{Y\})$-coordinates is ambiguous. Any coordinates belonging to the same set of irreducible representations of the isodynamic group, which describes the totality of vibrations, can be used to construct the PES. For this reason, the number of vibrations with a given type of coupling is independent of the choice of coordinates. To determine the Hamiltonian of a nonrigid N-atomic molecule, the frequency of ϕ-vibration at the PES minimum, $3N - 7$ frequencies ω_k of transverse $\{Y\}$ vibrations, $3N - 7$ coefficients of ϕY-couplings, and $(3N - 6)(3N - 7)/2$ coefficients of Asq- and YY'-couplings should be calculated.

The difference between the set of $(\phi,\{Y\})$-coordinates and the $(\xi,\{\eta\})$ moving frame (Fig. 3) used in the reaction path Hamiltonian formalism[20] should be emphasized. The large-amplitude coordinate ξ is chosen to be directed along a tangent to the MEP, while $3N - 7$ $\{\eta\}$-coordinates are chosen to be directed normal to the MEP. The use of the moving frame simplifies calcula-

Table 1. Bond lengths (d) and planar and dihedral angles (φ) in the ground and transition states of the HNO_3 molecule

Parameters	State	
	ground*	transition
Bond	d/Å	
H–O(1)	0.969 (0.964)	0.966
N–O(1)	1.407 (1.406)	1.449
N–O(2)	1.213 (1.211)	1.205
N–O(3)	1.202 (1.199)	1.205
Angle	φ/deg	
H–O(1)–N	102.04 (102.15)	101.813
O(1)–N–O(2)	115.67 (115.88)	114.625
O(1)–N–O(3)	113.70 (113.85)	114.625
O(2)–N–O(3)	130.63 (130.27)	130.685
O(2)–N–O(1)–H	0.0	−91.299
O(3)–N–O(1)–H	180.0	91.299

* Experimental data[1] are given in parentheses.

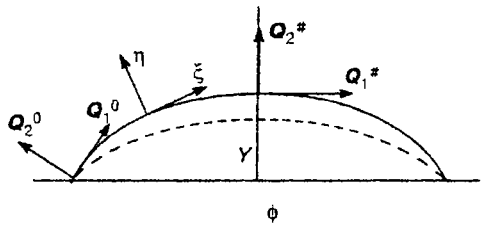

Fig. 3. System of generalized coordinates for a nonrigid molecule. A two-dimensional section including the reactive and gated transverse coordinates. Solid line is the minimum energy path (MEP), dashed line is the extreme tunneling trajectory; (ξ, η) is the frame moving along the MEP; (Q_1^0, Q_2^0) and ($Q_1^{\#}$, $Q_2^{\#}$) are the eigenvectors of normal vibrations in the ground and transition state, respectively.

tions in cases where the ETT approaches the MEP, which occurs if the frequencies of transverse vibrations are higher than that of ϕ-vibration. However, in the case of low-frequency vibrations the ETT strongly deviates from the MEP and has a highly curved portion that can hardly be taken into account using the above-mentioned formalism.[20]

Let us denote the eigenvectors of normal vibrations in the ground and transition states as Q^0 and $Q^{\#}$, respectively. For vibrations with Hl-couplings, the system of $(\phi,\{Y\})$-coordinates does not coincide with the $Q^{\#}$ set, which distinguishes this case from other types of couplings. In the vicinity of stationary points $\phi = \phi^{\#}$ and $\phi = \phi^0$ the potential function $V(\phi, \{Y\})$ and the classical kinetic energy $T(p_\phi, \{p_Y\})$ become quadratic forms of coordinates $(\phi - \phi^{\#}, \{Y - Y^{\#}\})$ and $(\phi - \phi^0, \{Y - Y^0\})$ and corresponding conjugate momenta $(p_\phi{}^{\#}, \{p_Y{}^{\#}\})$ and $(p_\phi{}^0, \{p_Y{}^0\})$. Let us introduce $(3N - 6)\times(3N - 6)$ matrices of transformation of these coordinates into normal ones:

$$Q^{\#} = P^{\#}(\phi - \phi^{\#}, \{Y - Y^{\#}\}),\ Q^0 = P^0(\phi - \phi^0, \{Y - Y^0\}). \quad (8)$$

Once the matrix S of transformation of Q^0- and $Q^{\#}$-coordinates is defined,

$$Q^0 = SQ^{\#}; \quad (9)$$

then, taking into account relationships (8), we get:

$$Q^{\#} = P^{\#}(P^0)^{-1}Q^0,\ S = P^{\#}(P^0)^{-1}. \quad (10)$$

The problem of determining the elements of the $P^{\#}$ and P^0 matrices and the above-listed parameters of the Hamiltonian is inverse to the eigenvalue problem for normal vibrations. Since the matrices V and T are diagonal in $Q^{\#}$ and Q^0 coordinates, diagonalization of these pairs of quadratic forms provides a set of equations for determination of the PES parameters. It is convenient to choose the dihedral angle (a natural coordinate corresponding to change in the geometry element) as ϕ-coordinate.

It is possible to unambiguously find a set of $\{Y\}$-coordinates such that 1) the kinematic matrix $G^{\#}$ is a unit matrix for all types of vibrations; 2) the force matrix $F^{\#}$ is a diagonal Jordan supermatrix whose diagonal blocks correspond to vibrations of different symmetry; 3) the blocks of $F^{\#}$ matrix, corresponding to Bre- and Hga-vibrations, are diagonal, so the eigenfrequencies and eigenvectors of these vibrations coincide with $\Omega_k{}^{\#}$ and $Q_k{}^{\#}$, respectively; 4) the blocks of $F^{\#}$ matrix, corresponding to ϕ- and Hl-vibrations, contain off-diagonal elements equal to the coefficients of ϕY-couplings; and 5) off-diagonal elements of YY'-couplings in $F^{\#}$ are equal to zero. The above-listed conditions follow from the shapes of two-dimensional sections of the PES, defined by formulas (1) and (2), and take into account the fact that the coordinates belonging to the same irreducible representation of the isodynamic group can be chosen to be mutually orthogonal. In the ground state the force and kinematic matrices become non-diagonal; in the case of kinematic matrix G^0 this is due to ϕ-dependent kinematic couplings. Using formulas (9) and (10) and taking into account that $P^{\#}\tilde{P}^{\#} = \hat{1}$, we get

$$G^0 = (\tilde{P}^0)^{-1}(P^0)^{-1} = \tilde{S}(\tilde{P}^{\#})^{-1}(P^{\#})^{-1}S = \tilde{S}S, \quad (11)$$

where $\tilde{P}^0$ and $\tilde{S}$ are transposed matrices.

The diagonal elements in the force matrix F^0 are due to Asq-couplings, while the appearance of off-diagonal elements is due to ϕY- and YY'-couplings. Using $(3N - 6)$ known frequencies $\Omega_k{}^{\#}$, from a total of $(3N - 5)(3N - 6)$ transformation equations of quadratic forms $G^{\#}$ and $F^{\#}$ it is possible to find $(3N - 6)^2$ elements of the $P^{\#}$ matrix and $3N - 6$ frequencies of ϕ- and $\{Y\}$-vibrations, which characterize the PES. Using relationships (10), the transformation equations of G^0 are transformed into identities, while from $(3N - 5)(3N - 6)/2$ transformation equations of F^0 it is possible to determine $3N - 7$ coefficients of C-couplings, $3N - 7$ coefficients of Asq-couplings, and $(3N - 7)(3N - 8)/2$ coefficients of YY'-couplings, *i.e.*, $(3N - 6)(3N - 5)/2$ parameters. Thus, the number of transformation equations is sufficient to determine all the necessary PES parameters.

The outlined procedure for calculation of parameters of the Hamiltonian has a drawback consisting of neglect of higher terms of the expansion in powers of the tunneling coordinate. The differences of the squares of the frequencies appearing in the secular equations are proportional to the squares of the coefficients of ϕY- and YY'-couplings and to the first degree of coefficients of Asq-couplings, so the solutions of the secular equations are slightly dependent on the coefficients of ϕY-coupling making the main contribution to the action and the higher-order anharmonicity corrections affect, the accuracy of C_k determination. Therefore, it is necessary to use another method for determining the C_k values, taking into account the dependence of $(\phi^{\#} - \phi^0)$ and $\{Y^{\#} - Y^0\}$ on internal deformation of the molecule.

For Bre-, Hl-, and Hga-vibrations, changes in Y_k-coordinates of the ground state with respect to those of the transition state (ΔY_k) are related to the coupling constants by the formula

$$C_k = \omega_k^2 \Delta Y_k, \qquad (12)$$

which provides $3N - 7$ equations for all types of coupling. The coefficients C_k are linearly related to ΔY_k, so the accuracy of their determination using formula (12) is higher than in the case of solving the inverse problem.

Comparison of the geometries of the equilibrium and distorted transition states makes it possible to find the displacements along transverse coordinates ΔY_k and then to calculate the coupling constants C_k using formula (12). The results are listed in Table 2. The elements of the S matrix are listed in Table 3. The matrix P^0 is found using relationships (10) and is used to

Table 2. Frequencies (ν/cm^{-1}), amplitudes of zero vibrations ($\Delta Y/Å\ amu^{1/2}$), coupling constants (C/ω), and contributions to the action (W^*) in $H^{14}N^{16}O_3$, $H^{15}N^{16}O_3$, $H^{16}O^{14}N^{18}O_2$, $H^{18}O^{14}N^{16}O_2$, and $D^{14}N^{16}O_3$ molecules

Vibration	Number	Coupling	ΔY	ν^0/ν^a	ω	C/ω	W^*
HO	1	Bre	−0.008	3799/3843	10.783	0.101	−0.005
stretching			−0.009	3799/3843	10.783	0.109	−0.006
			−0.006	3787/3830	10.747	0.077	−0.003
			−0.008	3799/3843	10.783	0.101	−0.005
			−0.008	2766/2798	10.610	0.063	−0.002
NO	2	Hl	−0.027	1904/1902	5.335	0.161	0.001
antisymmetric			−0.016	1861/1859	5.217	0.090	0.0
stretching			−0.001	1903/1902	5.337	0.006	0.0
			−0.005	1873/1867	5.238	0.032	0.0
			−0.005	1892/1902	7.212	0.028	0.0
HON	3	Bre	−0.057	1366/1350	3.788	0.242	−0.025
bending			−0.051	1365/1337	3.753	0.214	−0.020
			−0.090	1359/1348	3.782	0.381	−0.063
			−0.055	1358/1332	3.739	0.227	−0.022
			−0.070	1056/1024	3.884	0.216	−0.020
NO	4	Bre	−0.074	1350/1291	3.622	0.298	−0.038
symmetric			−0.078	1333/1284	3.604	0.314	−0.042
stretching			−0.080	1349/1288	3.614	0.324	−0.045
			−0.107	1307/1259	3.532	0.421	−0.075
			−0.013	1352/1329	5.038	0.053	−0.001
NO_2	5	Bre	0.138	919/862	2.419	−0.373	−0.055
deformation			0.130	907/849	2.384	−0.346	−0.047
			0.015	910/859	2.410	−0.040	−0.001
			0.175	895/837	2.350	−0.458	−0.082
			0.058	918/861	3.266	−0.150	−0.009
NO_2	6	Hga	−0.115	770/719	2.009	0.258	−0.042
out-of-plane			−0.116	750/700	1.963	0.254	−0.040
			−0.141	768/715	2.007	0.314	−0.062
			−0.114	762/708	1.988	0.253	−0.040
			−0.088	769/672	2.549	0.177	−0.020
NO′	7	Bre	0.256	676/642	1.800	−0.513	−0.095
stretching			0.253	676/641	1.799	−0.506	−0.093
			0.208	654/618	1.733	−0.401	−0.057
			0.248	658/629	1.764	−0.488	−0.086
			0.191	671/633	2.400	−0.361	−0.051
ONO′	8	Hl	−0.248	596/604	1.572	0.433	0.052
bending			−0.257	594/602	1.559	0.445	0.056
			−0.083	587/592	1.644	0.153	0.006
			−0.299	580/585	1.486	0.495	0.075
			−0.061	556/601	2.270	0.109	0.002
HO	9	T	—	461/i471	—	—	—
torsional			—	461/i471	—	—	—
			—	459/i469	—	—	—
			—	460/i470	—	—	—
			—	341/i345	—	—	—

Table 3. S_{ij}-Matrix (9) for HNO_3 molecule (i,j = 0, 1, ..., 8)

j	i								
	0	1	2	3	4	5	6	7	8
0	0.99	0.00	0.00	−0.06	0.00	0.16	0.04	0.03	0.02
1	−0.12	0.76	0.16	0.00	0.32	0.28	0.41	0.05	0.02
2	−0.03	−0.18	0.22	0.12	−0.22	0.11	0.07	0.21	−0.04
3	−0.01	0.00	−0.07	1.03	−0.47	0.12	0.12	0.11	−0.06
4	−0.04	0.00	0.00	0.28	0.91	0.11	−0.15	−0.01	0.05
5	−0.10	0.00	0.00	0.00	0.00	0.99	0.05	0.00	0.00
6	0.24	−0.24	−0.01	−0.18	0.28	−0.15	0.72	0.04	−0.08
7	0.18	−0.12	−0.27	−0.04	0.22	−0.10	−0.07	0.82	−0.02
8	0.17	−0.08	0.00	0.15	0.00	−0.34	0.04	0.12	0.82

determine the coefficients of kinematic couplings listed in Table 4, in which the coefficients of totally symmetric Asq-couplings are also listed. The calculated normal frequencies of all vibrations (see Table 2), except for ν_1 and ν_2, differ from experimental data[2] by factors from 1.015 to 1.045, which gives a negligible correction to the action. Though the error of calculations of the ν_1 and ν_2 frequencies is 7 to 12%, the contribution of corresponding vibrations to the action is so small that this drawback also becomes insignificant.

The next step in the PES reconstruction is to determine the parameters of the 1D-potential. Taking into account all potential and kinematic couplings, the normal frequencies of the ν_9 torsional vibration in the ground and transition states (461 and i471 cm^{-1}, respectively) correspond to frequencies of 476 cm^{-1} and i532 cm^{-1} at the minimum and maximum of the 1D-potential, respectively. The difference in the magnitudes of these frequencies indicates a contribution of higher Fourier components. However, the total amplitude of the latter does not exceed 0.03. Neglecting these components and choosing the average value of the frequencies found above (Ω_0 = 504 cm^{-1}) as the characteristic frequency of the cosine barrier, we get the PES in the form (1) with dimensionless frequencies of the 1D-potential, equal to $\sqrt{2}$ and $i\sqrt{2}$, respectively.

Table 4. Potential (α_{kk}) and kinematic ($g_{kk'}$) couplings in HNO_3

Vibration	Quantum number	α_{kk}/ω_k	g_{kk}	g_{k0}
HO torsional	n	—	0.01	—
		—	0.01	—
		—	0.01	—
		—	0.01	—
		—	0.03	—
NO′ stretching	n_1	0.198	−0.03	0.0
		0.200	−0.04	0.0
		0.215	−0.06	0.0
		0.167	−0.02	0.0
		0.300	0.11	0.0
NO_2 deformation	n_2	0.330	0.01	0.0
		0.335	0.01	0.0
		0.298	0.04	0.0
		0.332	−0.01	0.0
		0.445	−0.01	0.0
NO symmetric stretching	n_3	0.341	0.33	0.0
		0.278	0.46	0.0
		0.351	0.12	0.0
		0.277	0.30	0.0
		0.175	0.01	0.0
HON bending	n_4	0.089	−0.05	0.0
		0.157	−0.04	0.0
		0.062	−0.05	0.0
		0.146	−0.02	0.0
		0.241	−0.01	0.0
HO stretching	n_5	−0.243	0.0	0.0
		−0.243	0.0	0.0
		−0.241	0.0	0.0
		0.243	0.0	0.0
		−0.245	0.0	0.0
ONO′ bending	n_6	−0.045	−0.22	0.0
		−0.045	−0.22	0.0
		−0.029	−0.21	0.0
		−0.036	−0.22	0.0
		−0.325	−0.28	0.0
NO antisymmetric stretching	n_7	0.008	−0.15	0.0
		0.008	−0.15	0.0
		0.006	−0.12	0.0
		0.036	−0.17	0.0
		−0.077	−0.05	0.0
NO_2 out-of-plane	n_8	0.313	0.14	0.10
		0.292	0.14	0.10
		0.307	0.14	0.10
		0.311	0.14	0.10
		0.788	0.14	0.05

The moment of inertia of internal rotation I in the HNO_3 molecule is $1.337 \cdot 10^{-40}$ g cm^2 ($2.60 \cdot 10^{-40}$ g cm^2 for DNO_3) and the Ω_0 value of 504 cm^{-1} corresponds to a height of the 1D-barrier of 3035 cm^{-1}. According to quantum-chemical calculations, the energy difference between the equilibrium transition state and the ground state of the HNO_3 molecule, *i.e.*, the adiabatic barrier height, V_{ad}, is 2657 cm^{-1}. As follows from the PES shape, the height of the 1D-cosine potential barrier V_0 is related to V_{ad} by the formula

$$V_{ad} = V_0\left(1 - 0.5\sum_{k=1}^{5}\frac{C_k^2}{\omega_k^2} + 0.5\sum_{k=6,7}\frac{C_k^2}{\omega_k^2} - \frac{C_8^2}{2\omega_8^2}\right). \qquad (13)$$

Unlike other couplings, HI-couplings do not change the barrier height; however they increase the effective length of the ETT, *i.e.*, the semiclassical parameter γ. On going to dimensionless variables this increase in γ is equivalent to increase in the adiabatic barrier height, *i.e.*, to inclusion of the third term in Eq. (13). Substitution of the coupling coefficients found in formula (13) gives a height of the 1D-barrier (V_0) of 3346 cm^{-1}, which is 300 cm^{-1} higher than that calculated above from the Ω_0 frequency. At the same time, at V_{ad} = 2657 cm^{-1} the adiabatic action $W_{ad} = 2\sqrt{2V_{ad}}I/\hbar$ is in good agreement with that found in the framework of PIA at V_0 = 3035 cm^{-1} (22.548 *vs.* 22.335, respectively). For this reason, further calculations were carried out using V_0 = 3035 cm^{-1} and Ω_0 = 504 cm^{-1}. With the above-mentioned PES parameters, the γ values for HNO_3 and DNO_3 molecules are 8.52 and 12.6, respectively.

The found fourth-fold nine-dimensional PES is used below to analyze tunneling dynamics in the framework of PIA. As follows from the data in Table 2, all transverse modes, except for two with the highest frequencies ν_1 and ν_2, are active and the coupling coefficients C_k/ω_k lie in the range from 0.20 to 0.50, so the number of variables in the dynamic problem cannot be less than seven. Moreover, strong couplings with ν_7 and ν_8 vibrations whose transverse frequencies are only higher than Ω_0 by factors from 1.6 to 1.8 make it impossible to use the adiabatic approximation usually employed for analyzing tunneling rotations.[8]

Calculations of tunneling splittings

Resonance between the ν_5 and $2\nu_9$ vibrations is a salient feature of internal rotation in the HNO_3 molecule. It is believed that Fermi resonances in rigid molecules are mainly caused by cross-anharmonicity of vibrations (see, *e.g.*, Ref. 21). If the energy difference between vibrational levels is of the same order of magnitude as the value of the matrix element of Fermi interaction F, the eigenvalues are determined by the Hamiltonian matrix of the two-level system. The same mechanism was also considered for nonrigid molecules, where the Fermi interaction causes mixing of symmetric and antisymmetric levels of doublets with closely lying energies, described by the Hamiltonians[3,21]:

$$H_{\pm} = \begin{vmatrix} E_{n0}^0 \pm \Delta_n^0 & F_{nn'} \\ F_{nn'} & E_{0n'}^0 \end{vmatrix}, \qquad (14)$$

where n and n' are respectively the quantum numbers of longitudinal and any transverse vibrations, and Δ_n^0 is the tunneling splitting of the nth level of torsional vibration; fundamental tunneling splitting of the level of resonant transverse vibration is neglected in this case. Relation (14) shows that Fermi interaction equalizes tunneling splittings and, consequently, band intensities of longitudinal and transverse vibrations. Both parameters (Δ_n^0 and $F_{nn'}$) can be determined from spectroscopic data.

To solve the dynamical problem is to find relations between Δ_n^0, $F_{nn'}$, and the PES parameters. The increase in tunneling splittings in the near-Fermi resonance regions can be explained[10] by mixing of the (n, n_k) and (n', $n_k - 1$) states ($n' - n = 1, 2, \ldots$) with close-lying energies due to ϕY-couplings. Since the wave functions of these states have the same exponents, the mixing consists in expanding the solutions of the transport equation for the pre-exponential factor into a perturbative series. The coefficients of this expansion in "pure" (n, n_k) states are inversely proportional to the energy differences between the states, so tunneling splittings increase as $(E_n - E_{n'})^{-2}$ in the near-resonance regions. Far beyond these regions the contributions of several states with different n' values become significant, so the two-level system approximation leading to Hamiltonian (14) is no longer valid. Fermi resonances affect tunneling splittings, causing, in particular, an anomalous isotope effect, *i.e.*, increase in the tunneling splittings in excited states upon replacement of a light isotope by a heavy one, due to change in the frequencies of resonant states.

In the framework of PIA the first-order ETT is found from solutions of the equations of motion for transverse coordinates using $\phi(t)$ for one-dimensional motion. In the case of periodic potential $V(\phi) = 0.5(1 - \cos(2\phi))$, $\sin\phi(t) = 1/\cosh t$ is used, while $Y_k(\phi)$ for vibrations with Bre-, HI-, and Hga-couplings are described as follows:

$$Y_k(\phi) = \begin{cases} -\dfrac{C_k}{2}\sin^2\phi\displaystyle\int_0^{\infty} e^{-\bar{\omega}_k z}\frac{A}{B}\,dz & \text{(Bre)} \\ g_{0k}\sin\phi - \dfrac{C_k + 2g_{0k}\bar{\omega}_k^2}{2\bar{\omega}_k}\sin\phi\displaystyle\int_0^{\infty} e^{-\bar{\omega}_k z}\frac{C}{B}\,dz & \text{(Hga), (15)} \\ -\dfrac{C_k}{\bar{\omega}_k^2}\cos\phi\left(\dfrac{1}{2} - \sin^2\phi\displaystyle\int_0^{\infty} e^{-\bar{\omega}_k z}\frac{A}{B^2}\,dz\right) & \text{(HI)} \end{cases}$$

where $A = \sinh z\cosh z$, $B = 1 + \sin^2\phi\sinh^2 z$, $C = \cosh z$, and $\bar{\omega}_k = \omega_k/\sqrt{2}$. Kinematic Bre- and HI- couplings change the ETT only in higher orders of expansion. In the case of 1D-potential, the action is equal to $2\sqrt{2}\gamma$.

Second-order corrections to the action due to transverse vibrations are additive and are calculated using the known procedure[9,10]:

$$\delta W_k^* = \begin{cases} -\dfrac{C_k^2}{2\sqrt{2}}\left(\tilde{\omega}_k\int_0^\infty e^{-\tilde{\omega}_k z} z\coth z\,dz - 1\right) & \text{(Bre)} \\ -\dfrac{(C_k + 2g_{0k}\tilde{\omega}_k^2)^2}{2\sqrt{2}\tilde{\omega}_k}\int_0^\infty e^{-\tilde{\omega}_k z}\dfrac{z}{\sinh z}\,dz + & \\ \quad + \dfrac{g_{0k}}{\sqrt{2}}(C + g_{0k}\tilde{\omega}^2) & \text{(Hga)}. \quad (16) \\ \dfrac{C_k^2}{8\sqrt{2}\tilde{\omega}^2}\left(\tilde{\omega}\int_0^\infty e^{-\tilde{\omega}_k z} z\coth z\,dz - 1\right) & \text{(Hl)} \end{cases}$$

As follows from formulas (16), Bre- and Hga-vibrations reduce the action, thus enhancing tunneling, whereas Hl-vibrations suppress it. The values of the second-order corrections to the action due to transverse vibrations are listed in Table 2.

In the framework of PIA the tunneling splittings can be calculated using the generalized Lifshitz–Herring formula as perturbative expansions in powers of tunneling splittings of pure states.[10] For instance, for the (0, 1)-state of the Bre-vibration we have

$$\Delta_{0\ldots1\ldots} = \Delta^{(0)}_{0\ldots1\ldots} + \left(\frac{C_k}{\omega_k}\right)^2\left[\frac{2\omega_k}{\gamma(2\sqrt{2}+\omega_k)}\frac{\Delta^{(0)}_{2\ldots0\ldots}}{(\omega-2\sqrt{2})^2} + \right.$$
$$\left. + \frac{\omega_k(\omega_k+\sqrt{2})^2}{\gamma^3(\omega_k+2\sqrt{2})^2(\omega_k+4\sqrt{2})^2}\frac{\Delta^{(0)}_{4\ldots0\ldots}}{(\omega_k-4\sqrt{2})^2} + \cdots\right], \quad (17)$$

where

$$\Delta^{(0)}_{n\ldots n_k\ldots} = 3\hbar\Omega_0\frac{2^{\frac{7}{2}n+\frac{7}{4}}\gamma^{n+\frac{1}{2}}}{\sqrt{2\pi n!}}\exp[-\gamma(2\sqrt{2}+\delta W^*)]. \quad (18)$$

From relationships (17) and (18) it follows that even slight mixing leads to increase in the tunneling splittings for excited states of transverse vibrations as compared to those for the ground state, due to substantial increase in the $\Delta^0_{n\ldots nk\ldots}$ values with increasing n. Asq-couplings cause no mixing; however, they contribute to the exponent, which is independent of γ and is proportional to the first degree of the coupling constant.[10] The contribution of α_{kk}-couplings is taken into account analogously and leads to the following relationship:

$$\Delta_{n\{n_k\}} = \Delta^{(0)}_{n\{n_k\}}\prod_k\left(\frac{v_k^0}{v_k^{\neq}}\right)^{n_k}\exp\left[\alpha_{kk}n_k\frac{\pi^2}{16(1+\tilde{\omega}_k)}\right]. \quad (19)$$

Results and Discussion

The three-dimensional section of the ETT, found from the system of equations (15) and describing displacements along the ν_6, ν_7, and ν_8 coordinates, is shown in Fig. 4. Since, according to Eqs. (1) and (2), displacements along the Bre-, Hga-, and Hl-coordinates have periods of π and 2π, the projections of the ETT portions $[0, \pi/2]$, $[\pi/2, \pi]$, $[\pi, 3\pi/2]$, and $[3\pi/2, 2\pi]$ on the planes of these vibrations are different and form a complex three-dimensional curve.

The results of calculations of tunneling splittings, listed in Table 5, are in good agreement with the experimental data for the HNO_3 molecule, which provides the possibility of reliable prediction of anomalous isotope effects in isotopomers. The ν_1 and ν_2 vibrations with the highest frequencies are inactive. Since for ν_1 the Asq-coupling is negative, tunneling splitting in the $1\nu_1$ state is smaller than in the ground state. Resonance between ν_2 and $4\nu_9$ vibrations slightly affects the splitting because of weak coupling. The group of vibrations at ν_6, ν_7, and ν_8 is due to different types of ϕY-coupling (Fig. 5, *a*). The $1\nu_6$ Hga-vibration interacts with the $1\nu_9$ vibration, while the $1\nu_8$ Hl-vibration interacts with the $2\nu_9$ vibration. Both levels corresponding to these ($1\nu_6$ and $1\nu_8$) vibrations are far off resonance and are split only slightly. Splitting of the $1\nu_7$ vibrational level is ~40 times as much as in the ground state because of mixing with the $2\nu_9$ vibration and strong potential coupling. The $1\nu_3$ and $1\nu_4$ vibrations are far off resonance; however, they interact with both the $2\nu_9$ and $4\nu_9$ vibrations, which, taking into account rather large coupling coefficients, leads to appreciable splittings. Of particular interest is the $1\nu_5$ vibrational level; almost exact resonance between this and the $2\nu_9$ vibration results in a splitting which is three orders of magnitude larger than that in the ground state.

Isotope substitution of heavy nuclei slightly changes relative frequencies of vibrations (*i.e.*, positions of resonances); however, it has a pronounced effect on the coupling constants. This is due to the fact that each normal vibration is a combination of different stretching, bending, and deformation vibrations of the same symme-

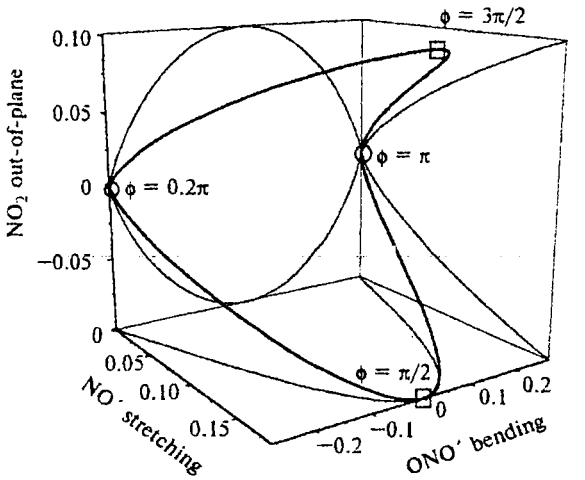

Fig. 4. Three-dimensional section of ETT in the HNO_3 molecule. The ETT projections on the planes are shown by thin lines.

Table 5. Calculated and experimental[3–7] tunneling splittings (cm^{-1}) of the zero and lowest excited vibrational levels of the HNO_3 molecule and its isotopomers

State	$H^{14}N^{16}O_3$	$H^{15}N^{16}O_3$	$H^{18}O^{14}N^{16}O_2$	$H^{14}N^{16}O^{18}O_2$	DNO_3	HNO_3 (experimental[3–7])
0	$8.53 \cdot 10^{-7}$	$7.97 \cdot 10^{-7}$	$5.28 \cdot 10^{-7}$	$8.91 \cdot 10^{-7}$	$9.50 \cdot 10^{-11}$	$\sim 10^{-7}$
$1\nu_9$	$7.58 \cdot 10^{-5}$	$7.02 \cdot 10^{-5}$	$4.40 \cdot 10^{-5}$	$8.99 \cdot 10^{-5}$	$2.00 \cdot 10^{-9}$	$6.66 \cdot 10^{-5}$
$2\nu_9$	$1.84 \cdot 10^{-3}$	$2.05 \cdot 10^{-3}$	$1.66 \cdot 10^{-3}$	$2.45 \cdot 10^{-3}$	$1.16 \cdot 10^{-7}$	$1.69 \cdot 10^{-3}$
$1\nu_8$	$9.60 \cdot 10^{-6}$	$9.84 \cdot 10^{-6}$	$3.07 \cdot 10^{-6}$	$1.61 \cdot 10^{-5}$	$5.42 \cdot 10^{-11}$	—
$1\nu_7$	$3.33 \cdot 10^{-5}$	$3.02 \cdot 10^{-5}$	$9.52 \cdot 10^{-5}$	$2.60 \cdot 10^{-5}$	$1.34 \cdot 10^{-8}$	—
$1\nu_6$	$3.54 \cdot 10^{-6}$	$3.46 \cdot 10^{-6}$	$2.93 \cdot 10^{-6}$	$3.68 \cdot 10^{-6}$	$2.02 \cdot 10^{-11}$	—
$1\nu_5$	$1.23 \cdot 10^{-3}$	$7.64 \cdot 10^{-4}$	$1.61 \cdot 10^{-5}$	$9.16 \cdot 10^{-4}$	$5.02 \cdot 10^{-10}$	$1.18 \cdot 10^{-3}$
$1\nu_4$	$4.48 \cdot 10^{-5}$	$4.73 \cdot 10^{-5}$	$3.38 \cdot 10^{-5}$	$1.09 \cdot 10^{-4}$	$1.83 \cdot 10^{-9}$	—
$1\nu_3$	$3.26 \cdot 10^{-5}$	$2.25 \cdot 10^{-5}$	$6.12 \cdot 10^{-5}$	$2.83 \cdot 10^{-5}$	$5.48 \cdot 10^{-9}$	—
$1\nu_2$	$4.70 \cdot 10^{-6}$	$3.28 \cdot 10^{-6}$	$9.24 \cdot 10^{-7}$	$2.57 \cdot 10^{-6}$	$1.99 \cdot 10^{-10}$	—
$1\nu_1$	$7.48 \cdot 10^{-7}$	$7.51 \cdot 10^{-7}$	$7.02 \cdot 10^{-7}$	$7.48 \cdot 10^{-7}$	$8.02 \cdot 10^{-11}$	—

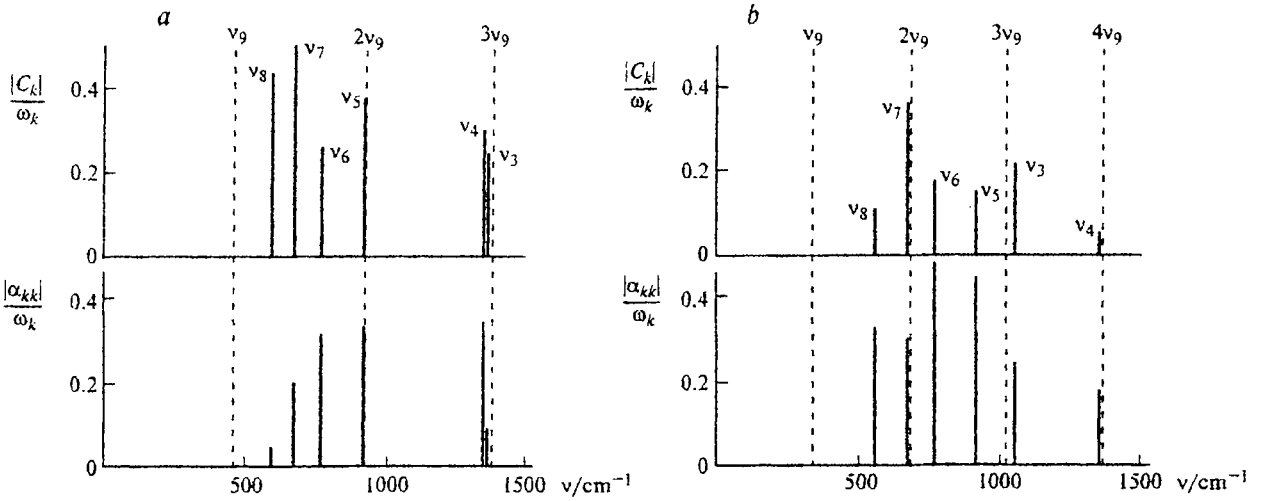

Fig. 5. Coefficients of potential and Asq-couplings in vibrational spectra of HNO_3 (*a*) and DNO_3 (*b*) molecules.

try. For instance, the NO_2 bending vibration, dominating at ν_5, is strongly mixed with the NO′ stretching vibration and HON bending vibration. Almost no mixing occurs in the $H^{18}O(N^{16}O_2)$ isotopomer, which is the reason for appreciable decrease in the coupling constant C and, as a consequence, for substantial decrease in the tunneling splitting. Unlike the isotopomers considered, resonances for the DNO_3 molecule are appreciably shifted (see Fig. 5). The frequency of the ν_9 vibration decreases by a factor of $\sim\sqrt{2}$, whereas other frequencies remain unchanged, except for ν_7 and ν_3 vibrations associated with the motion of the H(D) atom. The vibration at ν_4 appears to be almost resonant with the $4\nu_9$ vibration (see Fig. 5, *b*) and, despite the very weak coupling, splitting of the $1\nu_4$ vibrational level is ~60 times greater than that of the ground-state level. The vibration at ν_5 goes far beyond the resonance region, which decreases the splitting. The $1\nu_7$—$2\nu_9$ resonance occurs for the DNO_3 molecule instead of the $1\nu_5$—$2\nu_9$ one for HNO_3; the splitting of the $1\nu_7$ vibrational level is ~140 times greater than that of the ground-state level.

Using Table 5, it is possible to trace other changes in the splittings in isotopomers of the HNO_3 molecule. The $^{18}O'/^{16}O'$ substitution decreases the splitting in the ground state by a factor of 1.6, whereas substitution of the other two atoms only slightly increases it. The maximum $^{15}N/^{14}N$ isotope effect is observed for the $1\nu_5$ vibrational level, whose splitting decreases by a factor of 1.61. Splittings of the $1\nu_3$, $1\nu_7$, and $1\nu_8$ vibrational levels exhibit anomalous $^{18}O'/^{16}O'$ isotope effects (they increase by factors of 1.88 and 2.86 and decrease by a factor of 3.13, respectively). Violation of the $1\nu_5$—$2\nu_9$ resonance due to this substitution decreases the splitting by a factor of 75, whereas the isotope effect for the other two O atoms is only 0.75.

In conclusion let us note that the procedure suggested in this work can be applied to a great variety of complex nonrigid molecules with one large-amplitude coordinate. Analysis of tunneling dynamics in the HNO_3 molecule, taken as an example, shows that the vibrational-tunneling spectrum is well reproduced in the framework of PIA even in the presence of isolated

Fermi resonances. It is hoped that combination of quantum-chemical calculations and PIA will provide a universal approach to the analysis of molecular rearrangements in most of the nonrigid molecules and molecular complexes studied to date.

This work was supported by the Russian Foundation for Basic Research (Project No. 97-03-33687a).

References

1. A. P. Cox and J. M. Riveros, *J. Chem. Phys.*, 1965, **42**, 3106.
2. G. E. McGrow, D. L. Bernitt, and I. C. Hisatsune, *J. Chem. Phys.*, 1965, **42**, 237.
3. T. M. Goyette, C. D. Paulse, L. C. Oesterling, F. C. de Lucia, and P. Helminger, *J. Mol. Spectrosc.*, 1994, **167**, 365.
4. A. Perrin, J.-M. Flaud, C. Camy-Peyret, B. P. Wiknewisser, S. Klee, A. Goldman, F. J. Murcray, R. D. Blatherwick, F. S. Bonomo, D. G. Muiracray, and C. P. Rinsland, *J. Mol. Spectrosc.*, 1994, **166**, 224.
5. L. H. Coudert and A. Perrin, *J. Mol. Spectrosc.*, 1995, **172**, 352.
6. T. M. Goyette, L. C. Osterling, D. T. Petkie, R. A. Booker, P. Helminger, and F. C. de Lucia, *J. Mol. Spectrosc.*, 1996, **175**, 395.
7. C. D. Paulse, L. H. Coudert, T. M. Goyette, R. L. Grownover, P. Helminger, and F. C. de Lucia, *J. Mol. Spectrosc.*, 1996, **177**, 9.
8. V. A. Benderskii, D. E. Makarov, and C. A. Wight, *Chemical Dynamics at Low Temperatures*, Wiley Interscience, New York, 1994.
9. V. A. Benderskii, S. Yu. Grebenshchikov, E. V. Vetoshkin, L. von Laue, and H. P. Trommsdorff, *Chem. Phys.*, 1997, **219**, 119.
10. V. A. Benderskii, E. V. Vetoshkin, L. von Laue, and H. P. Trommsdorff, *Chem. Phys.*, 1997, **219**, 143.
11. V. A. Benderskii, E. V. Vetoshkin, and H. P. Trommsdorff, *Chem. Phys.*, 1998, **234**, 153.
12. V. A. Benderskii and E. V. Vetoshkin, *Chem. Phys.*, 1998, **234**, 173.
13. V. A. Benderskii, E. V. Vetoshkin, S. Yu. Grebenshchikov, and H.-P. Trommsdorff, *Zh. Fiz. Khim.*, 1997, **71**, 1985 [*Russ. J. Phys. Chem.*, 1997, **71** (Engl. Transl.)].
14. V. A. Benderskii, E. V. Vetoshkin, and H.-P. Trommsdorff, *Zh. Fiz. Khim.*, 1998, **72**, 50 [*Russ. J. Phys. Chem.*, 1998, **72** (Engl. Transl.)].
15. V. A. Benderskii, E. V. Vetoshkin, and H.-P. Trommsdorff, *Zh. Fiz. Khim.*, 1998, **72**, 2202 [*Russ. J. Phys. Chem.*, 1998, **72** (Engl. Transl.)].
16. M. J. Frisch, G. W. Trucks, H. B. Schlegel, P. M. W. Gill, B. G. Johnson, M. A. Robb, J. R. Cheeseman, T. Keith, G. A. Petersson, J. A. Montgomery, K. Raghavachari, M. A. Laham, V. G. Zakrzewski, J. V. Ortiz, J. B. Foresman, J. Cioslowski, B. B. Stefanov, A. Nanayakkara, M. Challacombe, C. Y. Peng, P. Y. Ayala, W. Chen, M. W. Wong, J. L. Andres, E. S. Replogle, R. Gomperts, R. L. Martin, D. J. Fox, J. S. Binkley, D. J. DeFrees, J. Baker, J. P. Stewart, M. Head-Gordon, C. Gonzalez, and J. A. Pople, *GAUSSIAN 94*, Revision C. 4, Gaussian, Inc., Pittsburgh (PA), 1995.
17. V. A. Benderskii, *Izv. Akad. Nauk, Ser. Khim.*, 1999, No. 12 [*Russ. Chem. Bull.*, 1999, **48**, No. 12 (Engl. Transl.)].
18. V. A. Benderskii, E. V. Vetoshkin, and H.-P. Trommsdorff, *Zh. Fiz. Khim.*, 2000, in press [*Russ. J. Phys. Chem.*, 2000, in press (Engl. Transl.)].
19. E. B. Wilson, Jr., J. C. Decius, and P. C. Cross, *Molecular Vibrations. The Theory of Infrared and Raman Vibrational Spectra*, McGraw-Hill, New York, 1955.
20. W. H. Miller, N. C. Handy, and J. E. Adams, *J. Chem. Phys.*, 1980, **72**, 99.
21. C. H. Townes and A. L. Schawlow, *Microwave Spectroscopy*, McGraw-Hill, New York, 1955.
22. E. Herbst, G. Winnewisser, K. M. Yamada, D. J. DeFrees, and A. D. McLean, *J. Chem. Phys.*, 1989, **91**, 5905.

Received March 19, 1999